FGA: An Allometric Model for Revealing the Relationship Between Fractal Geometry and AGB Estimation

Zhenyang Hui, Shuanggen Jin, *Senior Member, IEEE*, Penggen Cheng, and Yao Yevenyo Ziggah

***Abstract*— Above-ground biomass (AGB) is an important indicator for studying and understanding the ecological environment. However, the traditional AGB estimation methods using terrestrial Light Detection and Ranging (LiDAR) data still suffer from biases for different tree species or forest sites as well as low accuracy using the tree metrics. To overcome these challenges, this article developed a novel model based on fractal geometry. First, a theory was built to reveal the relationship between fractal geometry and AGB estimation. To realize this, three different theories were involved, including fractal theory, traditional AGB estimation theory, and stem form factor theory. The allometric AGB estimation equation was then developed based on fractal geometry parameters (i.e., fractal dimension and intercept). To test the proposed model, 101 individual trees located at different forest sites with corresponding harvested reference AGBs were adopted. Experimental results show that the proposed model can achieve better AGB results when compared with traditional allometric equations built upon tree metrics. All the utilized accuracy indicators revealed that the proposed method was the best. Relative root-mean-square error (RMSE) was improved by 53%, 22%, and 18% when compared with traditional allometric models built upon diameter at breast height (DBH), tree height, and the combined two variables (DBH and tree height). Furthermore, the performance of the developed model was also analyzed toward different tree species and different leaves on or off conditions. Results indicated that the developed model can produce satisfactory performance.**

***Index Terms*— Above-ground biomass (AGB), allometric model, fractal geometry, terrestrial Light Detection and Ranging (LiDAR).**

Manuscript received 8 August 2023; revised 17 October 2023; accepted 18 November 2023. Date of publication 20 November 2023; date of current version 30 November 2023. This work was supported in part by the National Natural Science Foundation of China (NSF) under Grant 42161060, Grant 41801325, and Grant 41861052; in part by the Jiangxi Outstanding Youth Fund under Grant 20232ACB213017; in part by the Jiangxi Province Double Thousand Plan High-level Talents Project under Grant DHSQT42023002; in part by the China Post-Doctoral Science Foundation under Grant 2019M661858; and in part by the Natural Science Foundation of Jiangxi Province under Grant 20192BAB217010. *(Corresponding author: Penggen Cheng.)*

Zhenyang Hui and Penggen Cheng are with the Faculty of Geomatics, East China University of Technology, Nanchang 330013, China (e-mail: huizhenyang2008@ecut.edu.cn; pgcheng@ecut.edu.cn).

Shuanggen Jin is with the School of Surveying and Land Information Engineering, Henan Polytechnic University, Jiaozuo 454000, China, and also with Shanghai Astronomical Observatory, Chinese Academy of Sciences, Shanghai 200030, China (e-mail: sgjin@shao.ac.cn).

Yao Yevenyo Ziggah is with the Geomatic Engineering Department, University of Mines and Technology (UMaT), Tarkwa 237, Ghana (e-mail: yyziggah@umat.edu.gh).

Digital Object Identifier 10.1109/TGRS.2023.3335197

I. Introduction

FOREST is one important component of the terrestrial ecosystem, which plays a significant role in maintaining the global climate system, regulating global carbon balance, and slowing down the rise of greenhouse gas concentration [1], [2]. Nowadays, forest above-ground biomass (AGB) has become an important index to measure forest carbon sink capacity and evaluate forest carbon budget [3].

Traditional optical remote-sensing technology usually utilizes satellite images to estimate forest biomass. However, remote-sensing images only provide horizontal spectral information and cannot obtain vertical structure information for the forest. As a result, it is generally difficult to achieve accurate AGB estimation results in dense forest areas [4]. Compared with optical remote-sensing technology, Light Detection and Ranging (LiDAR) is an active remote-sensing technology, which has been developing rapidly in recent years. LiDAR can obtain the 3-D structure information of forests, and provide reflection intensity, number of echoes, waveform, and so on. Thus, LiDAR has been widely used in forest inventory and especially with the fast development of terrestrial LiDAR (TLS), point clouds acquired by multiscan mode can provide detailed 3-D information [5]. Nowadays, it has become a major means for measuring tree metrics and AGB estimation [2], [6], [7].

AGB estimation methods using TLS can be classified into two categories based on measurable structural parameters and individual tree volume and wood density. For the first category of methods, individual tree structural parameters need to be calculated. The relationship between tree parameters and referenced AGB values needs to be fit to build the corresponding AGB estimation model [8]. The most commonly used tree parameters are diameter at breast height (DBH) and tree height [3], [9]. In the method proposed by Altanzagas et al. [3], four kinds of allometric equations of AGB estimation were established based on DBH, DBH square, tree height, and a combination of DBH square and tree height, respectively. Analytical results showed that different AGB estimation models were suitable for different tree species, and the establishment of tree species-specific AGB models would be beneficial to accurately estimate biomass. Basuki et al. [10] established an AGB estimation based on DBH. R^2 between the estimated results and the measured results was up to 0.989. In addition to

DBH and tree height, the wood density parameter was added to the model developed by Chave et al. [11]. Experimental results showed that this revised model can improve the estimation accuracy of AGB. In addition to the allometrics equations built upon tree metrics, Wang et al. [12] presented a new indicator named LiDAR biomass index (LBI) for AGB estimation. The obtained results showed that comparative performance can be achieved based on LBI. However, LBI should be first calculated using point clouds of analytical trees.

The main challenge for these methods is that inaccurate tree parameters will lead to the propagation of errors, which will seriously affect the subsequential estimation accuracy of AGB models. For instance, the estimation of DBH is prone to error due to the occlusion influence of LiDAR data. Moreover, treetops are difficult to detect by TLS, resulting in a low estimation of tree height. Tree parameters with a low calculated accuracy will not help to generate an accurate AGB estimation model. Moreover, the established AGB estimation models generally cannot achieve satisfactory performance in terms of different species or under different forest environments. Existing studies have shown that established empirical models tended to underestimate biomass by more than 35% for large tropical trees and eucalypts [13], [14].

AGB estimation methods based on tree volume and wood density generally need to estimate the tree volume first with the AGB calculated by multiplying wood density [7], [15], [17]. The tree volume can be obtained by voxelization [18], [19] or by local cylinder fitting [20], [21], [22]. The wood density can be obtained by field measurement of the ratio of dry weight to fresh volume of tree samples, or by querying the global wood density database of tree species [23], [24]. Takoudjou et al. [7] divided the individual tree into three parts, including the stump, stem, and crown. Cylinder fitting was carried out respectively, and the volume of the tree was obtained by adding these three parts together. Subsequently, wood density obtained from the global wood density database was used to convert tree volume into biomass. Kükenbrink et al. [2] obtained the volume of trees by constructing a quantitative structural model (QSM), and the biomass of individual trees was obtained by multiplying the wood density. In their study, wood density was determined by the ratio of the dry weight of tree samples to the fresh volume of tree samples. The key to this method is to obtain the accurate volume of individual trees, but existing studies have shown that the volume estimation of small branches (diameter less than 7 cm) is prone to error [25]. To solve such problems, the volume expansion factor was adopted by Longuetaud et al. [26]. The volume expansion factor is the ratio of the volume of partial components to the volume of the whole individual tree. In the method proposed by Demol et al. [16], model construction and volume estimation were carried out for branches whose diameters were larger than 7 cm, and then the volume expansion factor was multiplied to obtain the volume of the whole individual tree. This helped in solving the problem that small branches are prone to volume estimation deviation. However, the accuracy of volume estimation using this method is only slightly better than that based on the QSM of individual trees. Thus, Demol et al. [16] suggested that it was better to further improve the accuracy of QSM construction, especially for twig reconstruction to improve the estimation accuracy of individual tree volume.

In addition to the difficulty of accurately obtaining the volume of individual trees, another major problem with such methods is how to obtain wood density. Wood density is often related to many factors such as the geographical locations, growing environments, and sunlight exposure conditions of individual trees [11]. Hence, it is error-prone when getting the wood density by searching the global wood density database directly according to the tree species. In addition, not all species density information is included in the global wood density database. Although wood density can be measured directly in the field, it has been shown that the field measurement of wood density is heavily affected by the field environments [27]. Also, the density of wood in different parts of an individual tree tends to be different [28].

To sum up, the main challenges of AGB estimation using TLS mainly include the following four aspects.

1) The current calculated tree metrics used for AGB estimation, such as DBH, tree height, and so on, cannot reflect the overall structure of the tree in 3-D space. As a result, AGB estimation cannot be obtained using the descriptors in a global perspective with higher accuracy.
2) The calculated tree metrics used for AGB estimation is generally prone to errors. For example, treetops cannot be acquired effectively using TLS. Clearly, inaccurate tree metrics cannot lead to accurate AGB estimation results.
3) Most traditional AGB estimation models are specific to particular tree species. As a result, when applied to different tree species, these models fail to provide satisfactory AGB estimation performance. In other words, the traditional models lack robustness and applicability across various tree species.
4) The traditional allometric equations are generally built based on tree metrics (DBH, tree height, and so on). Leaves on or off conditions have little influence on the traditional model estimation results. Therefore, it is necessary to conduct further research on how the conditions of leaves on and off affect AGB estimation.

To solve the enumerated challenges, this article constructs a novel model for revealing the relationship between fractal geometry and AGB estimation and tries to estimate AGB at tree level using fractal geometry parameters. The newly developed AGB estimation model is not species-specific and can be applied to any individual tree. To sum up, the main contributions of this study mainly include the following three aspects.

1) To propose a novel allometric model for AGB estimation based on fractal parameters.
2) To analyze the relationship of fractal dimension and intercept toward AGB.
3) To evaluate the applicability and accuracy of the proposed fractal geometry allometric (FGA) equation for AGB estimation under different leaves on and off conditions.

The remainder of this article is organized as follows. In Section II, the principle of the proposed theory using fractal geometry for estimating AGB is demonstrated. Meanwhile, the developed FGA equation is derived. Section III conducts experiments and analysis using the LiDAR datasets at tree level to access the applicability and accuracy of the proposed theory. Section IV gives a discussion on the relationship between fractal geometry parameters and AGB, the performance of the developed model toward different tree species, and the influence of leaves on and off conditions. Finally, a conclusion regarding AGB estimation based on fractal geometry is given in Section V.

II. Methodology

The derivation process of the proposed fractal geometry-based AGB estimation model is illustrated in Fig. 1. It can be found that three theories are involved in deriving the proposed fractal geometry-based AGB estimation equation. These include fractal theory, traditional AGB estimation theory and stem form factor theory. In fractal theory, two fractal geometry parameters, namely, fractal dimension (d_{MB}) and intercept ($\mathrm{Intercept}_{\mathrm{MB}}$) can be calculated by using a log–log linear regression to voxel sizes and corresponding number of voxels. Although the classical log-log linear model has been established before, this article mainly utilizes it for exploring the relationship between voxel and fractal parameters, which will be used for further evolution of the traditional stem form factor calculation. In traditional AGB estimation theory, a new allometric equation between $\mathrm{Intercept}_{\mathrm{MB}}$ and AGB is derived from the traditional allometric AGB estimation equation based on the power-law relationship between tree height and DBH, and the power-law relationship between DBH and fractal intercept. In stem form factor theory, stem form factor (F) can be calculated using stem-wood volume (V), parabolic height (h_p), and cross-sectional area (s_p). Here, V can be calculated as the sum of a series of voxels, while voxels can be represented as an allometric equation of fractal geometry parameters. Thus, the stem form factor can be further derived as a fractal geometry parameter-based equation. Thereafter, the proposed fractal geometry-based AGB estimation equation was derived by substituting F into the traditional allometric equation. By taking the logarithmic transformation, the theoretical relationship between AGB and fractal geometry parameters can be derived. To sum up, four main steps are included in this article as described in Sections II-A–II-D, respectively.

A. Fractal Geometry Parameter Calculation

Fractal geometry was first defined by Mandelbrot [29]. In fractal theory, the structure or shape of an object shows a similarity to the whole when observing at different scales [30]. It recognizes that changes in the dimension of space can be both discrete and continuous. Since fractal geometry provides a cheap way to access the structure and size of plants, it has been widely used in vegetation point extraction and tree metrics (DBH, height, crown area, and so on) estimation [30], [31], [32]. However, never has it been used for AGB estimation based on LiDAR datasets.

In general, the fractal parameters can be calculated according to the box-counting method, where the object can be covered by a series of boxes. In terms of 3-D point clouds, the box can be replaced as voxels. As shown in Fig. 2, the individual tree can be covered by voxels of different sizes.

By fixing the edge of a cube, we can achieve the optimal coverage of voxels for an individual tree. In practice, the initial cube edge is set to the maximum value of Δx, Δy, and Δz, Δx, Δy, and Δz refer to the differences between the maximum and minimum x, y, and z coordinates, respectively. In this case, we use one large voxel to cover the individual tree. As the cube edge is decreased, more voxels will be required to cover the individual tree and the number of voxels will increase exponentially. The voxelization is kept iterating until the cube edge is equal to the mean point spacing distance. A log–log linear regression can be built between voxel size and the number of voxels as defined in the following equation [30]:

$$\log N_1 = d_{\mathrm{MB}} \times \log\left(\frac{1}{\mathrm{Voxel}}\right) + \mathrm{Intercept}_{\mathrm{MB}} \tag{1}$$

where N_1 is the number of voxels and Voxel represents the voxel size. Obviously, different Voxel corresponds to different N_1. The relationship between them can be solved by linear regression with d_{MB} as the slope, which is also named as fractal dimension. The $\mathrm{Intercept}_{\mathrm{MB}}$ is the intercept of the linear model.

The coefficients d_{MB} and $\mathrm{Intercept}_{\mathrm{MB}}$ in the linear model can be calculated using the least-squares principle. As previously mentioned, the voxel size (Voxel) influences the number of voxels (N_1). By obtaining a series of values for Voxel and N_1, regression analysis can be used to calculate the coefficients d_{MB} and $\mathrm{Intercept}_{\mathrm{MB}}$. Regression analysis aims to find the optimal coefficients that minimize the residual sum of squares.

Equation (1) is a classical formula in fractal theory. Different from existing studies, this article further derived the relationship between Voxel and fractal geometry parameters based on (1) as follows:

$$\mathrm{Voxel} = \exp\left(\left(\mathrm{Intercept}_{\mathrm{MB}} - \log(N_1)\right)/d_{\mathrm{MB}}\right). \tag{2}$$

From (2), it is easy to find that voxel size is related to fractal information. This relationship will be used for further evolution of the traditional stem form factor calculation mentioned in Section II-C.

B. Evolution of the Traditional Allometric Equation

It is generally suggested that AGB should be proportional to DBH, tree height and specific wood density. Thus, a traditional allometric equation for AGB estimation is generally established as follows [33]:

$$\mathrm{AGB} = F \times \left(\rho \times \left(\frac{\pi D^2}{4}\right) \times H\right)^{\beta} \tag{3}$$

where F is the stem form factor, ρ is the specific wood density, D is DBH, and H is the tree height. β shows the power-law

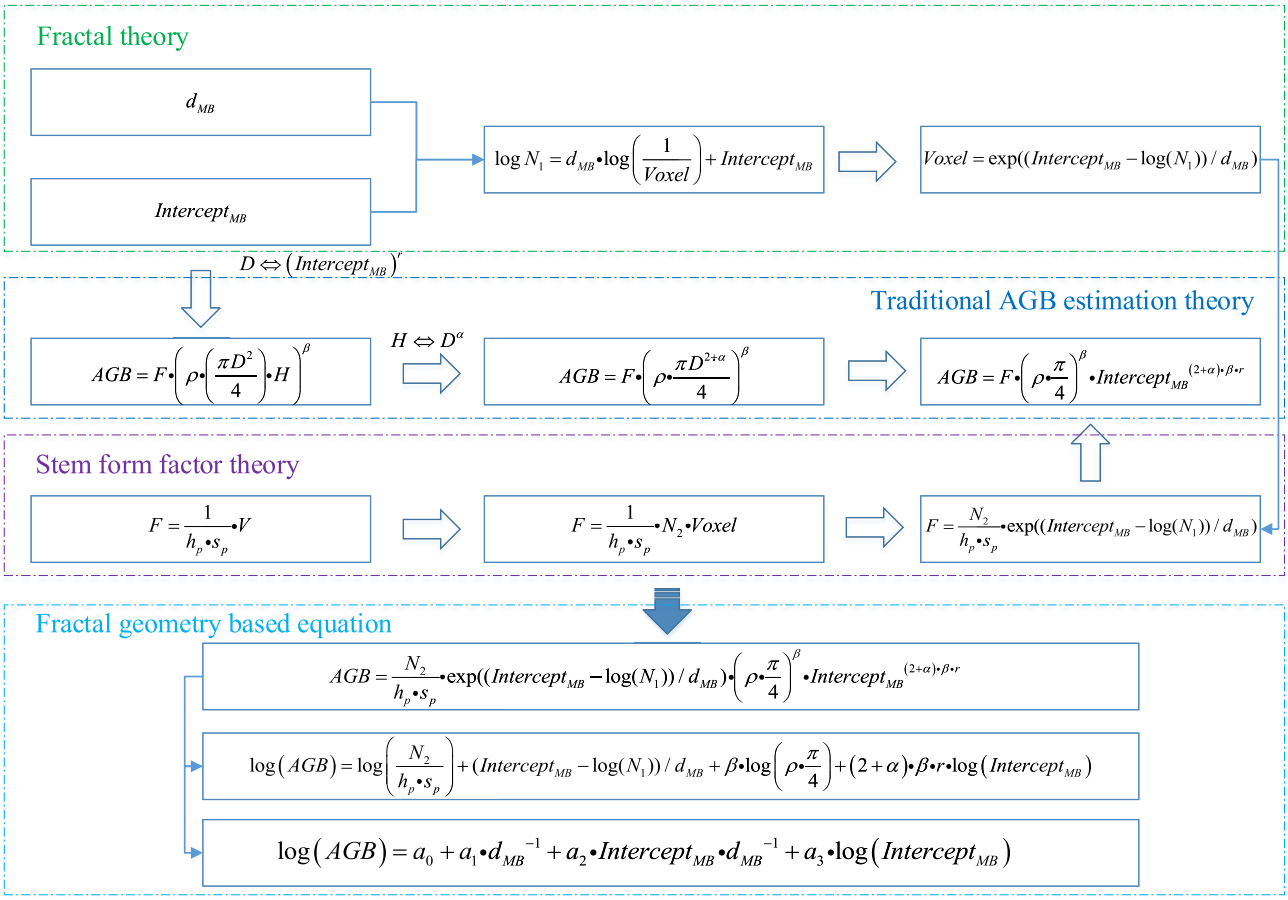

Fig. 1. Derivation of the proposed fractal geometry-based AGB estimation model.

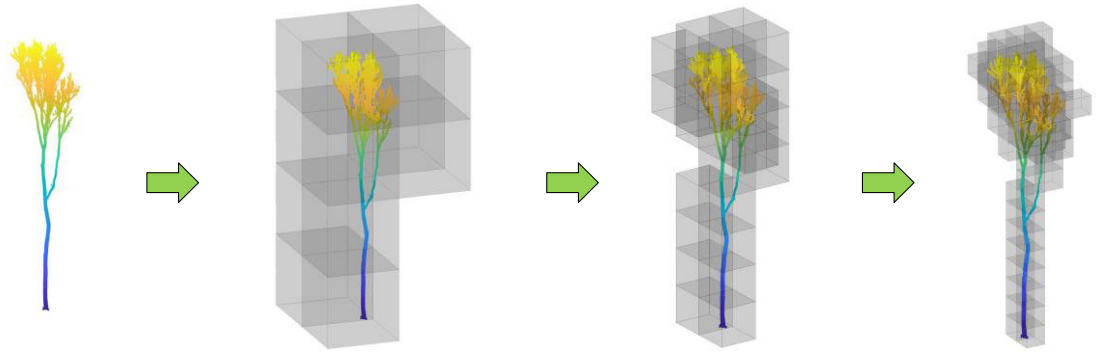

Fig. 2. Fractal geometry parameters calculation based on the box-counting method. With the gray voxel size changing smaller, the number of voxels increases distinctly.

relationship between AGB and the tree metrics. Due to the occlusion of the tree canopy, tree height is difficult to be measured by TLS. For better AGB estimation, (3) can be evolved as a DBH-based allometric equation as follows:

$$\mathrm{AGB} = F \times \left(\rho \times \frac{\pi D^{2+\alpha}}{4}\right)^{\beta}. \tag{4}$$

Equation (4) is derived based on the power-law relationship between tree height and DBH, that is $H \Leftrightarrow D^{\alpha}$ [34]. Here, $\Leftrightarrow$ represents proportionality. Furthermore, Guzmán et al. [30] have proven that fractal geometry parameters can be used to predict tree metrics. This is because there is a strong power-law relationship between DBH and $\mathrm{Intercept_{MB}}$. Here, we defined it as $D \Leftrightarrow \left(\mathrm{Intercept_{MB}}\right)^r$. Subsequently, (4) can be further derived as follows:

$$\mathrm{AGB} = F \times \left(\rho \frac{\pi}{4}\right)^{\beta} \times \mathrm{Intercept}_{\mathrm{MB}}^{(2+\alpha)\beta r}. \tag{5}$$

C. Stem Form Factor Calculation by Voxelization

From (5), it is easy to find that AGB is only related to the product of the stem form factor and one fractal geometry parameter. In general, the stem form factor is related to the proportions of tree branches to stems and varies among different forest types [34], [35].

In stem form factor theory, the shape of stem wood is assumed as a quadratic paraboloid [36]. Thus, the parabolic volume of the stem wood can be calculated as a product of parabolic height and cross-sectional area as defined in the following equation [35]:

$$V = F \times h_p \times s_p \tag{6}$$

where V is the wood volume, h_p is the parabolic height, and s_p is the cross-sectional area at the base of the paraboloid [35]. F is the stem form factor, which is affected by tree species. In general, when encountering with mature conifers, F will be smaller. On the contrary, when encountering with broadleaved trees, F will be larger [35]. Thus, it can be found that the stem form factor is difficult to determine. Different from existing studies, this article does not calculate F according to tree species. Instead, F is derived based on the wood volume, which can be estimated by voxelization. Thus, F can be further solved by the following equation:

$$F = \frac{1}{h_p \times s_p} \times N_2 \times \text{Voxel} \tag{7}$$

where N_2 is the number of voxels. Similar with (1), when voxel size changes smaller, the number of voxels will be increased as a power function.

D. Deviation of the Proposed FGA Equation

By substituting (2) and (7) into (5), a new model for AGB estimation can be derived as follows:

$$\text{AGB} = \frac{N_2}{h_p \times s_p} \exp\left(\left(\text{Intercept}_{\text{MB}} - \log(N_1)\right)/d_{\text{MB}}\right) \times \left(\rho\frac{\pi}{4}\right)^{\beta} \times \text{Intercept}_{\text{MB}}^{(2+\alpha)\beta r}. \tag{8}$$

By taking the logarithmic transformation, a log-log model can be achieved as follows:

$$\log(\text{AGB}) = \log\left(\frac{N_2}{h_p \times s_p}\right) + \left(\text{Intercept}_{\text{MB}} - \log(N_1)\right)/d_{\text{MB}} + \beta\log\left(\rho\frac{\pi}{4}\right) + (2+\alpha)\beta r\log\left(\text{Intercept}_{\text{MB}}\right). \tag{9}$$

Equation (9) can be further simplified as an allometric equation of fractal geometry parameters, which is named as FGA equation in this article, defined as follows:

$$\log(\text{AGB}) = a_0 + a_1 \times d_{\text{MB}}^{-1} + a_2 \times \text{Intercept}_{\text{MB}} \times d_{\text{MB}}^{-1} + a_3 \times \log\left(\text{Intercept}_{\text{MB}}\right) \tag{10}$$

where a_0, a_1, a_2, and a_3 are coefficients, which can be solved by regression. In this case, the least-squares method is used to calculate these four coefficients. The aim of regression analysis is to find the optimal coefficients that minimize the residual sum of squares between the estimated and referenced AGB values. At this point, the fractal geometry-based AGB estimation model has been established.

III. Experimental Results and Analysis

A. Experimental Datasets and Evaluation Metrics

To evaluate the performance of the proposed FGA model, eight publicly available datasets located in different areas were tested. The eight datasets covered seven different tree species, including Pinus sylvestris, Larix decidua, Fagus sylvatica, Fraxinus excelsior, Quercus petraea, Erythrophleum, and Pinus massoniana. The characteristics of the tested datasets are tabulated in Table I. Among them, five datasets were collected from Belgium, one from Germany, and two from China [16], [20]. The five datasets collected from Belgium were acquired using a RIEGL VZ-1000 or VZ-400 terrestrial laser scanner [16]. There are 15, 15, 5, 15, and 15 individual trees in each forest site, respectively. The angular sampling resolution is 0.04°, and the pulse repetition rate is 300 KHz [16]. The datasets were scanned between December 2017 and March 2018. The last three forest stands include 12, 12, and 12 individual trees, respectively. The point clouds were collected using a Z+F IMAGER 5010 (10,000 pixel/360°) or Z+F IMAGER 5010c (20,000 pixel/360°) laser scanner, which belongs to phase shift scanning mode. The point clouds were collected between March 2013 and October 2013. In total, there are 101 individual trees (54 trees with leaves and 47 trees without leaves) in the eight forest stands. All the individual trees were felled and the AGBs were destructively measured. The AGBs will serve as reference values for testing the performance of the developed AGB estimation model.

Five accuracy metrics were used for testing the performance of the proposed method, including mean bias (mBias), relative mean bias (rmBias), root-mean-square error (RMSE), relative RMSE (rRMSE), and coefficient of determination (R^2). The five accuracy metrics are defined in (11)–(15). The first four indicators demonstrate deviation of the estimated AGBs from the referenced AGBs. R^2 can be seen as a measurement of self-similarity and can reflect the model explanatory degree [30]

$$\text{mBias} = \sum_{i=1}^{N} \text{abs}\left(\text{AGB}_{\text{est}}^{i} - \text{AGB}_{\text{ref}}^{i}\right) \Big/ N \tag{11}$$

$$\text{rmBias} = \text{mBias}/\overline{\text{AGB}_{\text{ref}}} \tag{12}$$

$$\text{RMSE} = \sqrt{\sum_{i=1}^{N}\left(\text{AGB}_{\text{est}}^{i} - \text{AGB}_{\text{ref}}^{i}\right)^2 \Big/ N} \tag{13}$$

$$\text{rRMSE} = \text{RMSE}/\overline{\text{AGB}_{\text{ref}}} \tag{14}$$

$$R^2 = \frac{\sum_{i=1}^{N}\left(\text{AGB}_{\text{ref}}^{i} - \overline{\text{AGB}_{\text{ref}}}\right)^2 - \sum_{i=1}^{N}\left(\text{AGB}_{\text{ref}}^{i} - \text{AGB}_{\text{est}}^{i}\right)^2}{\sum_{i=1}^{N}\left(\text{AGB}_{\text{ref}}^{i} - \overline{\text{AGB}_{\text{ref}}}\right)^2} \tag{15}$$

where $\text{AGB}_{\text{est}}^{i}$ is the ith estimated AGB using the developed model, while $\text{AGB}_{\text{ref}}^{i}$ is the referenced value. N is the total number of trees. $\overline{\text{AGB}_{\text{ref}}}$ is the mean referenced AGB value.

TABLE I
CHARACTERISTICS OF THE TESTED DATASETS [16], [20]

Site	Species	Laser scanner	Leaf/needle condition	Number of trees	Mean DBH (cm)	Mean tree height (m)
P.sylA (Belgium)	Pinus sylvestris	VZ-1000	Needle-on	15	21	31
P.sylB (Belgium)	Pinus sylvestris	VZ-1000	Needle-on	15	23	31
Lx.dc (Belgium)	Larix decidua	VZ-400	Needle-off	5	21	27
F.syl (Belgium)	Fagus sylvatica	VZ-1000	Leaf-off	15	22	37
F.exc (Belgium)	Fraxinus excelsior	VZ-1000	Leaf-off	15	19	22
Pirmasens (Germany)	Quercus petraea	Z+F IMAGER 5010c	Needle-on	12	27	27
Baiyun forest farm (China)	Erythrophle-um	Z+F IMAGER 5010c	Leaf-on	12	22	17
Baiyun forest farm (China)	Pinus massoniana	Z+F IMAGER 5010	Leaf-off	12	21	15

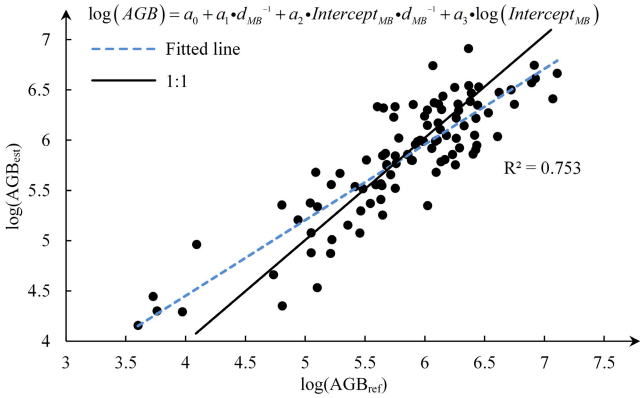

Fig. 3. Comparison between estimated AGBs and referenced AGBs. The black line is 1:1 line, while the blue dotted line is the fit line.

B. Experimental Results and Comparison

According to (10), the AGBs for the 101 individual trees can be estimated. If the estimated AGBs are all equal to the referenced AGBs, the points should be distributed along the least squares line of best fit designated as 1:1 in Fig. 3. In that case, all the estimated results are completely correct. In other words, if more points are distributed around the 1:1 line, the performance of the developed model will be better. From Fig. 3, it can be found that there are many points found around the line of best fit. As a result, R^2 of the developed model in this article is 0.753 as produced by the fit line between the estimated AGBs and referenced AGBs. The higher R^2 indicates that higher similarity existed between the estimated AGBs and referenced AGBs. Thus, it can be concluded that the developed AGB estimation model performs well in terms of these 101 individual trees.

The commonly used models for AGB estimation are developed based on DBH [10], [37], [38], which is expressed as $\text{AGB} = aD^b$. Since some researchers assumed that there is a power-law relationship between tree height and DBH ($H \Leftrightarrow D^\alpha$) [34], the DBH-based AGB models can be transformed to be $\text{AGB} = aH^b$. Another kind of famous AGB estimation model is based on DBH and tree height simultaneously [3], [4], which is expressed as $\text{AGB} = aD^bH^c$. To obtain better AGB estimation results, an interaction item ($D * H$) can also be added. That is $\text{AGB} = aD^bH^c(DH)^d$. With the fast development of individual tree modeling methods, some researchers also used the tree volume (V) and wood density (ρ) to estimate the biomass. That is $\text{AGB} = aV^b\rho^c$. As commented by Altanzagas et al. [3], the first four allometric equations built upon DBH, tree height, and the combined two variables (DBH and height) are suitable for different tree species, and the establishment of tree species-specific AGB models would be beneficial to accurately estimate biomass. In other words, the first four AGB estimation models are generally species-specific. The last allometric equation is built based on tree volume and wood density. Tree volume can be obtained by voxelization or by local cylinder fitting. Wood density can be obtained by field measurement of the ratio of dry weight to fresh volume of tree samples, or by querying the global wood density database according to tree species. This model based on tree volume and wood density is commonly regarded as a reliable method for estimating AGB.

To objectively evaluate the performance of the proposed method, this article compared the accuracy metrics of the proposed FGA model and the ones of these traditional AGB estimation models. The comparison result is tabulated in Table II. From Table II, it can be found that the proposed FGA model performs the best no matter which accuracy indicator is adopted. In terms of R^2, the proposed method performs much better than the models based on one variable (D or H). For two variables (D and H) combined, the proposed method still outperformed the traditional models. In terms of RMSE, the proposed model still achieved the lowest value. rRMSE was improved 41.3, 10.2, 8.1, and 9.9 percentage points compared with traditional allometric models built upon DBH, tree height, and the combined two variables. Although the AGB estimation model based on tree volume was expected to achieve a promising result, its performance was still worse than the proposed model due to the poor wood density accuracy of different tree species.

TABLE II
COMPARISON WITH COMMONLY USED ALLOMETRIC MODELS

Allometric models	R^2	*mBias* (kg)	*rmBias*	*RMSE* (kg)	*rRMSE*
$AGB = aD^b$	0.318	172.241	0.420	320.538	0.782
$AGB = aH^b$	0.530	139.473	0.340	193.208	0.471
$AGB = aD^b H^c$	0.611	125.652	0.306	184.674	0.450
$AGB = aD^b H^c \left(DH\right)^d$	0.623	127.237	0.310	191.787	0.468
$AGB = aV^b \rho^c$	0.593	132.834	0.324	194.920	0.475
The proposed model	0.753	106.224	0.259	151.419	0.369

TABLE III
ESTABLISHED AGB MODELS AND CORRESPONDING EQUATIONS [39]. *N* IS THE NUMBER OF TREES IN THE TESTED PLOT, *D* IS DBH (CM), *H* IS TREE HEIGHT (M), AND WD IS WOOD DENSITY (G/CM^3)

Models	Sample data range	AGB Equations	Forest type	Region
Sandra *et al.* [33]	$n = 94$ DBH:5–130cm	$\exp(-2.409 + 0.9522 * \ln(DBH^2 * H * WD))$	Moist forest	Pantropical
Li [40]	$n = 102$ DBH:5-80cm	$0.042086 * (DBH^2 * H)^{0.970315}$	Moist forest	Hainan, China
MKetterings *et al.* [38]	$n = 29$ DBH:7.6–48.1cm	$0.066 * D^{2.59}$	Secondary forest	Sumatra, Indonesia
Chave *et al.*[34]	$n = 1504$ DBH:5–156cm	$0.0509 * (DBH^2 * H * WD)$	Moist forest	Pantropical
Kenzo *et al.* [41]	$n = 136$ DBH:0.1–20.7cm	$0.0829 * D^{2.43}$	Secondary forest	Sarawak, Malaysia
Chan *et al.* [42]	$n = 160$ DBH:0.1–20.7cm	$0.063 * \left(D^2 * H\right)^{0.862}$	Secondary forest	Bago, Myanmar
Chave *et al.* [11]	$n = 4004$ DBH: 5–156cm	$0.0673 * (DBH^2 * H * WD)^{0.976}$	Moist forest	Pantropical

TABLE IV
ACCURACY METRICS FOR THE ESTABLISHED ALLOMETRIC EQUATIONS

Models	R^2	*mBias* (kg)	*rmBias*	*RMSE* (kg)	*rRMSE*
Sandra *et al.*[33]	-0.018	390.427	0.952	1733.643	4.229
Li [40]	-0.230	500.645	1.221	2110.783	5.149
MKetterings *et al.* [38]	-0.385	825.414	2.013	4921.392	12.005
Chave *et al.*[34]	0.125	347.672	0.848	1774.576	4.329
Kenzo *et al.* [41]	-0.239	523.164	1.276	2711.893	6.615
Chan *et al.* [42]	0.223	237.938	0.580	743.702	1.814
Chave *et al.* [11]	0.073	361.347	0.881	1741.840	4.249

Many established AGB equations have also been built for specific species or local regions as shown in Table III. To further analyze the performance of the proposed method, this article computed the accuracy metrics according to these established AGB equations as listed in Table III and their corresponding obtained results are shown in Table IV. From

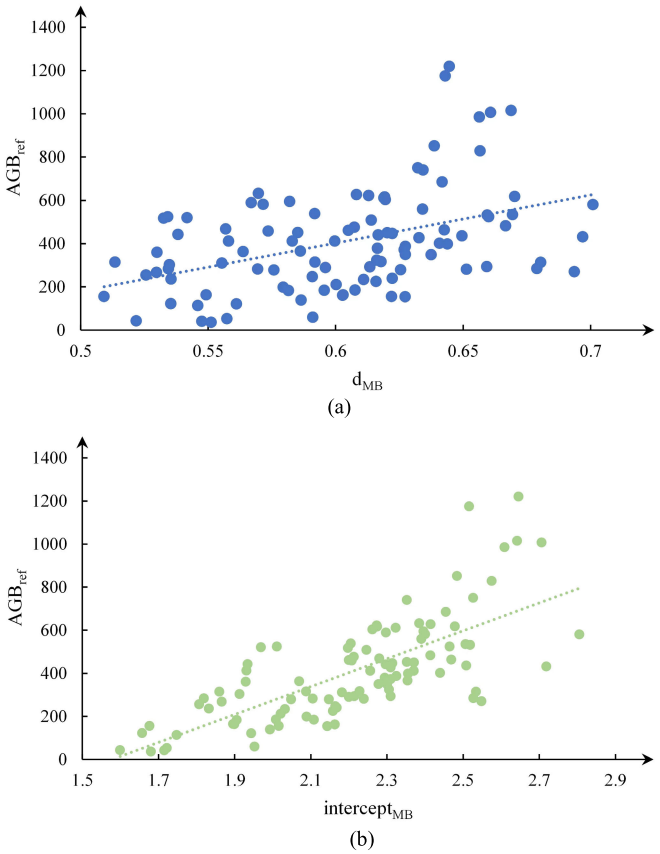

Fig. 4. Relationship between fractal geometry parameters and referenced AGBs: (a) d_{MB} and referenced AGBs and (b) Intercept_{MB} and referenced AGBs.

Table III, it can be found that these seven AGB estimation equations were developed toward different forest types and different regions. Using these established equations for testing will help to show the robustness and applicability of the established models toward the 101 trees tested in this study.

Table IV demonstrates that when testing these 101 trees, all seven established AGB equations showed poorer performance. All the R^2 values were smaller or even negative. It means that the estimated AGBs by the five established equations have little similarity with the referenced AGBs. The smallest mBias (237.938 kg) was achieved by Chan et al. [42], which is more than two times that of the proposed model (106.224 kg, Table II). Meanwhile, the largest mBias (825.414 kg) was about eight times that of the proposed model. In terms of RMSE, the proposed method also performed much better. The reasons for the bad performance of these established models are twofold. The first is that the measurement of DBH and tree heights generally involves errors. This is because the measured DBH always relies on circle fitting. Hence, the calculated result is easily prone to error. In terms of tree height, LiDAR pulses may miss actual treetops. Studies have also shown that the field-measured wood density can easily produce errors [27]. Moreover, these established equations are generally built upon trees in specific regions or of specific species. When applying these existing models to other datasets, good performance cannot be guaranteed.

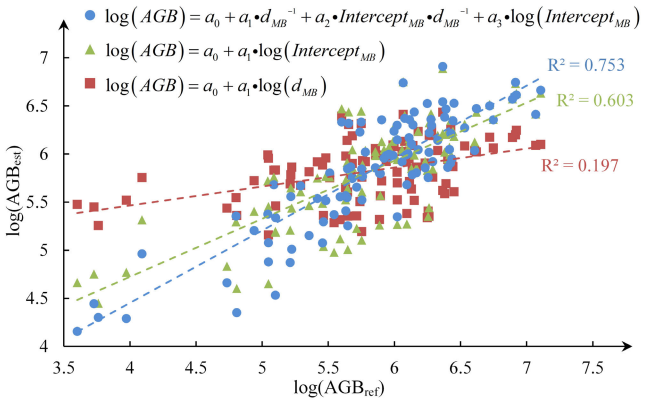

Fig. 5. Comparison of AGB estimation models based on fractal geometry parameters.

IV. Discussion

A. Relationship Between Fractal Geometry Parameters and AGB

Fig. 4 shows the relationship between fractal geometry parameters and referenced AGBs. From Fig. 4(a) and (b), it can be found that both d_{MB} and Intercept_{MB} have the growing tendency with referenced AGBs changing to be larger. However, this tendency is not obvious as indicated by the fit lines shown in Fig. 4(a) and (b). The largest referenced AGBs do not own the highest d_{MB} and it is the same for Intercept_{MB}. In terms of d_{MB}, its value varies from 0 to 1. For the tested datasets used in this article, d_{MB} values are mainly between 0.55 and 0.65 [Fig. 4(a)]. In general, d_{MB} close to 0 represents a cylindrical tree. Since most trees have branches and canopies, d_{MB} values are generally larger than 0. This can also be found in Fig. 4(a). Conversely, d_{MB} close to 1 represents that the tree points are uniformly occupied the 3-D space [30]. In other words, the individual tree is regular in shape like a Menger sponge. It must be admitted that most trees do not meet this requirement in nature. That is why d_{MB} values are generally smaller than 1. In terms of Intercept_{MB}, its values can be positive and negative. In general, larger objects own larger Intercept_{MB} values [30]. Thus, a tree with larger size generally owns larger Intercept_{MB}. This is why Intercept_{MB} values have a tendency to increase as the referenced AGB values become larger, as illustrated in Fig. 4(b).

As the dotted line shown in Fig. 4(a) and (b), both d_{MB} and Intercept_{MB} have a growing tendency when referenced AGBs changes to be larger. It seems that there could be a relationship between d_{MB} or Intercept_{MB} and AGB. To verify this, this article developed two AGB estimation models based on only one variable (d_{MB} or Intercept_{MB}) and tested their estimation performance. Fig. 5 shows the comparison results with the proposed model in this article. From Fig. 5, it can be found that Intercept_{MB} can be better used for AGB estimation than d_{MB}. Comparing with d_{MB} or Intercept_{MB}-based models, the proposed model performs much better. R^2 of the proposed model is the highest. More importantly, the allometric equation developed in this article is derived step by step and not obtained by roughly combining the two fractal geometry parameters.

TABLE V
PERFORMANCE OF THE DEVELOPED MODEL TOWARD DIFFERENT TREE SPECIES

Species	R^2	*mBias* (kg)	*rmBias*	*RMSE* (kg)	*rRMSE*
Pinus massoniana	0.609	37.181	0.225	42.210	0.255
Erythrophleum fordii	0.902	30.569	0.090	37.041	0.109
Quercus petraea	0.576	50.926	0.105	60.051	0.124
Pinus sylvestris	0.888	58.595	0.130	82.051	0.182
Larix decidua	0.989	6.122	0.016	9.008	0.024
Fraxinus excelsior	0.929	78.883	0.230	104.373	0.305
Fagus sylvatica	0.441	136.994	0.228	172.827	0.288
AVE	0.762	57.038	0.146	72.509	0.184

TABLE VI
ACCURACY METRICS COMPARISON TOWARD THE DEVELOPED MODEL UNDER LEAF-ON AND LEAF-OFF CONDITIONS. *N* IS THE NUMBER OF TREE

Leaf condition	*N*	Tree height (m)	DBH (cm)	R^2	*mBias* (kg)	*rmBias*	*RMSE* (kg)	*rRMSE*
Leaf on	54	19.227±3.812	27.650±7.236	0.790	67.499	0.186	93.186	0.257
Leaf off	47	22.010±3.538	36.089±28.210	0.740	131.279	0.283	174.263	0.375
Leaf on and off	101	20.522±3.925	31.577±20.291	0.753	106.224	0.259	151.419	0.369

B. Performance of the Developed Model Toward Different Tree Species

To verify the robustness of the developed AGB estimation model toward different tree species, this article tested the datasets separately by species. As shown in Table I, there are seven tree species in these datasets, namely, Pinus massoniana, Erythrophleum fordii, Quercus petraea, Pinus sylvestris, Larix decidua, Fraxinus excelsior, and Fagus sylvatica. The AGB estimation performance using the developed model toward these tree species is tabulated in Table V. It can be found that the developed model performs well in most species. Six out of eight tree species can achieve R^2 larger than 0.6. As a result, the average R^2 of all these seven species is 0.762, which means that promising AGB estimation results can be achieved by this article. In terms of mBias, only one tree species' mBias is larger than 100 kg. It means the proposed method can obtain the estimated biomass results as accurately as the referenced values. Moreover, almost all the rRMSEs of tree species are smaller than 30%. Thus, it can be concluded that the developed AGB estimation model has strong robustness toward different tree species. However, it is important to note that the performance of the proposed model varies for different tree species. For instance, the R^2 value for Fagus sylvatica is 0.441, while the R^2 value for Larix decidua is 0.989. One of the main reasons for this discrepancy is the limited number of tree samples used to test the accuracy of AGB estimation in this study. In the case of Fagus sylvatica, only 15 tree samples were available. Additionally, these samples exhibited a wide range of referenced AGB values, ranging from 350.062 to 1175.124 kg. Consequently, constructing a reliable AGB estimation model using such a small number of diverse tree samples becomes challenging.

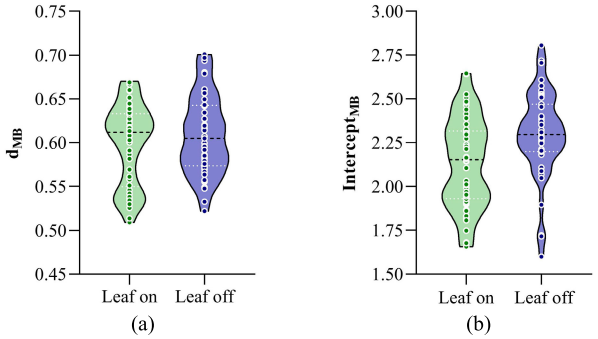

Fig. 6. Violin plot comparing fractal geometry parameters under different leaf conditions: (a) d_{MB};d_{MB} and (b) $Intercept_{MB}$. The black dotted line represents the median, while the two white dotted lines represent 25 percentile and 75 percentile, respectively.

C. Influence of Leaf-On and Leaf-Off Conditions

As presented in Table I, among the tested 101 individual trees there are 54 trees with leaves and 47 trees without leaves. To further analyze the influence of leaves on and off conditions on the developed model, this article calculated fractal geometry parameters and accuracy metrics, respectively. The fractal geometry parameters calculation results are shown in Fig. 6. From Fig. 6(a), it can be found that trees with leaves tend to have larger d_{MB} values larger than 0.6. As a result, the median d_{MB} value [black dotted line in Fig. 6(a)] of trees with leaves is higher than that of trees without leaves. This can be explained by the fact that trees with leaves cover more voxels, resulting in a greater occupation of 3-D space when calculating the fractal dimension. As mentioned previously, when a tree evenly occupies its space, its fractal dimension will be larger. Fig. 6(b) shows $Intercept_{MB}$ values distribution under different leaf conditions. It can be found that most

trees without leaves tend to have larger $\text{Intercept}_{\text{MB}}$ values. Examining Table VI, the heights of trees without leaves are higher than the trees with leaves in this study. Meanwhile, DBHs of trees without leaves are also larger than the trees with leaves in this study. This means that trees without leaves are larger in size than trees with leaves in the testing datasets. As mentioned in Section IV-A, a tree with a larger size generally has large $\text{Intercept}_{\text{MB}}$. That is why the $\text{Intercept}_{\text{MB}}$ values of trees without leaves tend to be higher than the trees with leaves.

Table VI presents the accuracy metrics of the developed model under different leaf conditions. It can be observed that no matter leaf on or leaf off, the proposed model can achieve good AGB estimation performance. All the R^2 are larger than 0.7. In this study, trees with leaves can achieve the smallest mBias and *RMSE* values. This is because trees with leaves in this study tend to have smaller DBHs. More importantly, DBHs exhibit smaller changes (27.650 $\pm$7.236 cm) among the trees with leaves when compared with the trees without leaves (36.089 $\pm$28.210 cm). As a result, mBias and RMSE values for the trees without leaves are about two times the ones with leaves. This indicates that the proposed model tends to achieve better AGB estimation result when the trees are smaller in size.

V. Conclusion

This article proposed a new allometric model for AGB estimation. Unlike traditional allometric models built upon tree metrics (DBH, tree height, and so on), the proposed model applies fractal geometry parameters (d_{MB} and $\text{Intercept}_{\text{MB}}$) for estimating AGB from a global perspective. The strengths of the newly built model are twofold. On the one hand, the developed model provides a new way of estimating AGB, which will not need the prerequisite of tree metrics calculation. Compared to the newly proposed LBI indicator, the calculation of fractal geometry parameters is much easier and does not need to calculate the leaf area of each crown layer. In addition, the developed model is not species-specific, which extends its application to any tree species for AGB estimation. To test the proposed model, 101 individual trees collected from eight different forest sites are used to assess the performance of the proposed model. The datasets include seven different tree species and contain 54 trees with leaves and 47 trees without leaves, respectively. Experimental results show that the developed model can achieve good AGB performance. Compared with the traditional tree metrics-based models, the proposed model achieved the highest R^2 and lowest mBias and RMSE. Moreover, the relationship between fractal geometry parameters and AGB estimation shows that combining d_{MB} with $\text{Intercept}_{\text{MB}}$ performed better than the single variable-based model. Furthermore, the developed model was tested on the trees with and without leaves. Experimental results show that the proposed model can achieve good AGB results in both leaves on and off conditions. The newly developed AGB estimation model could provide a new way for researchers and make more contributions to the forest inventory. However, it is still uncertain whether the fractal geometry parameters can be utilized for estimating AGB on a large scale. In our forthcoming research, we will concentrate on estimating regional AGB using the principles of fractal geometry.

References

[1] M. I. Disney et al., "Weighing trees with lasers: Advances, challenges and opportunities," *Interface Focus*, vol. 8, no. 2, Apr. 2018, Art. no. 20170048, doi: 10.1098/rsfs.2017.0048.

[2] D. Kükenbrink, O. Gardi, F. Morsdorf, E. Thürig, A. Schellenberger, and L. Mathys, "Above-ground biomass references for urban trees from terrestrial laser scanning data," *Ann. Botany*, vol. 128, no. 6, pp. 709–724, Oct. 2021, doi: 10.1093/aob/mcab002.

[3] B. Altanzagas, Y. Luo, B. Altansukh, C. Dorjsuren, J. Fang, and H. Hu, "Allometric equations for estimating the above-ground biomass of five forest tree species in Khangai, Mongolia," *Forests*, vol. 10, no. 8, p. 661, Aug. 2019, doi: 10.3390/f10080661.

[4] D. Xu, H. Wang, W. Xu, Z. Luan, and X. Xu, "LiDAR applications to estimate forest biomass at individual tree scale: Opportunities, challenges and future perspectives," *Forests*, vol. 12, no. 5, p. 550, Apr. 2021, doi: 10.3390/f12050550.

[5] Z. Dong et al., "Registration of large-scale terrestrial laser scanner point clouds: A review and benchmark," *ISPRS J. Photogramm. Remote Sens.*, vol. 163, pp. 327–342, May 2020, doi: 10.1016/j.isprsjprs.2020.03.013.

[6] B. Brede et al., "Non-destructive estimation of individual tree biomass: Allometric models, terrestrial and UAV laser scanning," *Remote Sens. Environ.*, vol. 280, Oct. 2022, Art. no. 113180, doi: 10.1016/j.rse.2022.113180.

[7] S. M. Takoudjou et al., "Using terrestrial laser scanning data to estimate large tropical trees biomass and calibrate allometric models: A comparison with traditional destructive approach," *Methods Ecol. Evol.*, vol. 9, no. 4, pp. 905–916, Apr. 2018, doi: 10.1111/2041-210x.12933.

[8] S. M. Beyene, "Estimation of forest variable and aboveground biomass using terrestrial laser scanning in the tropical rainforest," *J. Indian Soc. Remote Sens.*, vol. 48, no. 6, pp. 853–863, Jun. 2020, doi: 10.1007/s12524-020-01119-2.

[9] Y. Xue, Z. Yang, X. Wang, Z. Lin, D. Li, and S. Su, "Tree biomass allocation and its model additivity for *Casuarina equisetifolia* in a tropical forest of Hainan island, China," *PLoS ONE*, vol. 11, no. 3, Mar. 2016, Art. no. e0151858, doi: 10.1371/journal.pone.0151858.

[10] T. M. Basuki, P. E. van Laake, A. K. Skidmore, and Y. A. Hussin, "Allometric equations for estimating the above-ground biomass in tropical lowland dipterocarp forests," *Forest Ecol. Manage.*, vol. 257, no. 8, pp. 1684–1694, Mar. 2009.

[11] J. Chave et al., "Improved allometric models to estimate the aboveground biomass of tropical trees," *Global Change Biol.*, vol. 20, no. 10, pp. 3177–3190, Oct. 2014, doi: 10.1111/gcb.12629.

[12] Q. Wang, Y. Pang, D. Chen, X. Liang, and J. Lu, "LiDAR biomass index: A novel solution for tree-level biomass estimation using 3D crown information," *Forest Ecology Manage.*, vol. 499, Nov. 2021, Art. no. 119542, doi: 10.1016/j.foreco.2021.119542.

[13] K. Calders et al., "Nondestructive estimates of above-ground biomass using terrestrial laser scanning," *Methods Ecol. Evol.*, vol. 6, no. 2, pp. 198–208, Feb. 2015, doi: 10.1111/2041-210x.12301.

[14] J. G. de Tanago et al., "Estimation of above-ground biomass of large tropical trees with terrestrial LiDAR," *Methods Ecology Evol.*, vol. 9, no. 2, pp. 223–234, Feb. 2018, doi: 10.1111/2041-210x.12904.

[15] A. E. L. Stovall, A. G. Vorster, R. S. Anderson, P. H. Evangelista, and H. H. Shugart, "Non-destructive aboveground biomass estimation of coniferous trees using terrestrial LiDAR," *Remote Sens. Environ.*, vol. 200, pp. 31–42, Oct. 2017, doi: 10.1016/j.rse.2017.08.013.

[16] M. Demol, K. Calders, H. Verbeeck, and B. Gielen, "Forest above-ground volume assessments with terrestrial laser scanning: A ground-truth validation experiment in temperate, managed forests," *Ann. Botany*, vol. 128, no. 6, pp. 805–819, Oct. 2021, doi: 10.1093/aob/mcab110.

[17] L. B. T. Sagang et al., "Using volume-weighted average wood specific gravity of trees reduces bias in aboveground biomass predictions from forest volume data," *Forest Ecol. Manage.*, vol. 424, pp. 519–528, Sep. 2018, doi: 10.1016/j.foreco.2018.04.054.

[18] F. Hosoi, Y. Nakai, and K. Omasa, "3-D voxel-based solid modeling of a broad-leaved tree for accurate volume estimation using portable scanning LiDAR," *ISPRS J. Photogramm. Remote Sens.*, vol. 82, pp. 41–48, Aug. 2013.

[19] M. R. McHale, "Volume estimates of trees with complex architecture from terrestrial laser scanning," *J. Appl. Remote Sens.*, vol. 2, no. 1, May 2008, Art. no. 023521.

[20] J. Hackenberg, M. Wassenberg, H. Spiecker, and D. Sun, "Non destructive method for biomass prediction combining TLS derived tree volume and wood density," *Forests*, vol. 6, no. 12, pp. 1274–1300, Apr. 2015, doi: 10.3390/f6041274.

[21] Z. Hui, Z. Cai, B. Liu, D. Li, H. Liu, and Z. Li, "A self-adaptive optimization individual tree modeling method for terrestrial LiDAR point clouds," *Remote Sens.*, vol. 14, no. 11, p. 2545, May 2022, doi: 10.3390/rs14112545.

[22] P. Raumonen et al., "Fast automatic precision tree models from terrestrial laser scanner data," *Remote Sens.*, vol. 5, no. 2, pp. 491–520, Jan. 2013, doi: 10.3390/rs5020491.

[23] J. Chave, D. Coomes, S. Jansen, S. L. Lewis, N. G. Swenson, and A. E. Zanne, "Towards a worldwide wood economics spectrum," *Ecol. Lett.*, vol. 12, no. 4, pp. 351–366, Apr. 2009.

[24] A. E. Zanne et al., *Global Wood Density Database*. Leicester, U.K.: Dryad, 2009. [Online]. Available: http://hdl.handle.net/10255/dryad.235

[25] M. Abegg, R. Boesch, M. E. Schaepman, and F. Morsdorf, "Impact of beam diameter and scanning approach on point cloud quality of terrestrial laser scanning in forests," *IEEE Trans. Geosci. Remote Sens.*, vol. 59, no. 10, pp. 8153–8167, Oct. 2021, doi: 10.1109/TGRS.2020.3037763.

[26] F. Longuetaud et al., "Modeling volume expansion factors for temperate tree species in France," *Forest Ecol. Manage.*, vol. 292, pp. 111–121, Mar. 2013.

[27] G. B. Williamson and M. C. Wiemann, "Measuring wood specific gravity-correctly," *Amer. J. Botany*, vol. 97, no. 3, pp. 519–524, Mar. 2010, doi: 10.3732/ajb.0900243.

[28] S. Patiño et al., "Branch xylem density variations across the Amazon Basin," *Biogeosciences*, vol. 6, pp. 545–568, Apr. 2009.

[29] B. B. Mandelbrot, *The Fractal Geometry of Nature*. New York, NY, USA: Freeman, 1983.

[30] J. A. Guzmán Q., I. Sharp, F. Alencastro, and G. A. Sánchez-Azofeifa, "On the relationship of fractal geometry and tree–stand metrics on point clouds derived from terrestrial laser scanning," *Methods Ecol. Evol.*, vol. 11, no. 10, pp. 1309–1318, Oct. 2020, doi: 10.1111/2041-210x.13437.

[31] D. Seidel, M. Ehbrecht, Y. Dorji, J. Jambay, C. Ammer, and P. Annighöfer, "Identifying architectural characteristics that determine tree structural complexity," *Trees*, vol. 33, no. 3, pp. 911–919, Jun. 2019, doi: 10.1007/s00468-019-01827-4.

[32] H. Yang, W. Chen, T. Qian, D. Shen, and J. Wang, "The extraction of vegetation points from LiDAR using 3D fractal dimension analyses," *Remote Sens.*, vol. 7, no. 8, pp. 10815–10831, Aug. 2015, doi: 10.3390/rs70810815.

[33] B. Sandra, A. Gillespie, and A. E. Lugo, "Biomass estimation methods for tropical forests with applications to forest inventory data," *Forest Sci.*, vol. 35, no. 4, pp. 881–902, 1989.

[34] J. Chave et al., "Tree allometry and improved estimation of carbon stocks and balance in tropical forests," *Oecologia*, vol. 145, no. 1, pp. 87–99, Aug. 2005.

[35] M. G. R. Cannell, "Woody biomass of forest stands," *Forest Ecol. Manage.*, vol. 8, nos. 3–4, pp. 299–312, Jun. 1984.

[36] H. R. Gray, *Principles of Forest Tree and Crop, Volume Growth: A Mensuration Monograph* (Bulletin Australia. Forestry and Timber Bureau), vol. 1. Jun. 1966, p. 42.

[37] S. Brown, "Estimating biomass and biomass change of tropical forests: A primer," *FAO Forestry Paper*, vol. 134, p. 87, Jan. 1997.

[38] Q. M. Ketterings, R. Coe, M. van Noordwijk, Y. Ambagau', and C. A. Palm, "Reducing uncertainty in the use of allometric biomass equations for predicting above-ground tree biomass in mixed secondary forests," *Forest Ecol. Manage.*, vol. 146, nos. 1–3, pp. 199–209, Jun. 2001.

[39] B. Liu, W. Bu, and R. Zang, "Improved allometric models to estimate the aboveground biomass of younger secondary tropical forests," *Global Ecol. Conservation*, vol. 41, Jan. 2023, Art. no. e02359, doi: 10.1016/j.gecco.2022.e02359.

[40] Y. Li, "Comparative analysis for biomass measurement of tropical mountain rain forest in Hainan Island, China," *Acta Ecolog. Sinica*, vol. 13, pp. 313–320, Jan. 1993.

[41] T. Kenzo et al., "Allometric equations for accurate estimation of above-ground biomass in logged-over tropical rainforests in Sarawak, Malaysia," *J. Forest Res.*, vol. 14, no. 6, pp. 365–372, Dec. 2009.

[42] N. Chan, S. Takeda, R. Suzuki, and S. Yamamoto, "Establishment of allometric models and estimation of biomass recovery of swidden cultivation fallows in mixed deciduous forests of the Bago Mountains, Myanmar," *Forest Ecol. Manage.*, vol. 304, pp. 427–436, Sep. 2013.

Zhenyang Hui was born in Kaifeng, Henan, China in 1989. He received the B.S. degree in surveying engineering from the Henan University of Engineering, Zhengzhou, Henan, China, in 2008, and the Ph.D. degree in geodesy and survey engineering from the China University of Geosciences, Wuhan, Hubei, China, in 2017.

From 2017 to 2020, he was a Lecturer, and since 2020, he has been an Associate Professor with the Faculty of Geomatics, East China University of Technology, Nanchang, China. He has authored more than 60 peer-reviewed journal articles. His research interests include Light Detection and Ranging (LiDAR) point clouds processing, artificial intelligence, machine learning, and pattern recognition.

Dr. Hui was awarded the best paper at the National LiDAR Conference in 2019 at Xiamen, China. He was a recipient of Jiangxi Province Outstanding Surveying and Mapping Geographic Information Technology Young Talents (2021), Jiangxi Province Double Thousand Plan High-Level Talents (2022), and Jiangxi Outstanding Youth Fund (2023).

Shuanggen Jin (Senior Member, IEEE) was born in Anhui, China, in 1974. He received the B.Sc. degree in geodesy from Wuhan University, Wuhan, China, in 1999, and the Ph.D. degree in geodesy from the University of Chinese Academy of Sciences, Beijing, China, in 2003.

He is currently a Vice President and a Professor with Henan Polytechnic University, Jiaozuo, China, and also a Professor with Shanghai Astronomical Observatory, CAS, Shanghai, China. He has over 500 articles in peer-reviewed journals and proceedings, ten patents/software copyrights and ten books/monographs with more than 9000 citations, and H-index $>$ 50. His main research areas include satellite navigation, remote sensing, space geodesy and space/planetary exploration.

Prof. Jin was a President of the International Association of Planetary Sciences (IAPS) from 2013 to 2017 and the International Association of CPGPS from 2016 to 2017, the Chair of IUGG Union Commission on Planetary Sciences (UCPS) from 2015 to 2023, a Vice President of the IAG Commission 2 from 2015 to 2019, a Vice Chair of COSPAR's Panel on Satellite Dynamics (PSD) from 2016 to 2020, and the *Advances in Space Research* from 2013 to 2017, and has been an Editor-in-Chief of the *International Journal of Geosciences* since 2010, an Associate Editor of IEEE TRANSACTIONS ON GEOSCIENCE AND REMOTE SENSING since 2014, the *Journal of Navigation* since 2014, a Editorial Board Member of the *GPS Solutions* since 2016, the *Journal of Geodynamics* since 2014, and the *Planetary and Space Science* since 2014. He has received one first-class and four second-class Prizes of Provincial Awards, 100-Talent Program of CAS in 2010, a fellow of IAG in 2011, Fu Chengyi Youth Sci. & Tech. Award in 2012, the Xia Jianbai Award of Geomatics in 2014, a member of the Russian Academy of Natural Sciences in 2017 and the European Academy of Sciences in 2018, an IUGG Fellow in 2019, a member of Academia Europaea in 2019 and the Turkish Academy of Sciences in 2020, the World Class Professor of Ministry of Education and Cultures, Indonesia in 2021, a fellow of Electromagnetics Academy, USA, in 2021, and so on.

Penggen Cheng was born in Nanchang, Jiangxi, China, in 1964. He received the B.S. degree in surveying engineering from the East China Institute of Geology, Fuzhou, Jiangxi, China, in 1985, the M.S. degree in photogrammetry and remote sensing from the Wuhan Technology University of Surveying and mapping, Wuhan, Hubei, China, in 1996, and the Ph.D. degree in photogrammetry and remote sensing from Wuhan University, Wuhan, Hubei, China, in 2005.

He was a Visiting Scholar with the University of Waterloo, Waterloo, ON, Canada, from 2008 to 2009. From 1985 to 2000, he was a Lecturer and an Associate Professor with the Surveying Department, East China Institute of Geology. Since 2000, he has been a Professor with the Faculty of Geomatics, East China University of Technology, Nanchang, China. He has authored four books and more than 180 articles. His research interests include geographic information system theory and software development, 3-D data model theory and application, remote sensing geomapping, and urban ecological environment monitoring.

Dr. Cheng was a recipient of the Yexue'an Excellent Teacher Award in 2017, a young and middle-aged expert with outstanding contributions from National Nuclear Industry Corporation of China in 1998, and an expert on special government allowances under the State Council in 2002. He is an Editor of the *Geography and Geographical Information Science*.

Yao Yevenyo Ziggah was born in Agona Ninta, Central Region, Ghana in 1984. He received the Bachelor of Science degree (Hons.) in geomatic engineering from the Kwame Nkrumah University of Science and Technology (KNUST), Kumasi, Ghana, in 2008, and the Master of Engineering and Doctor of Philosophy degrees in geodesy and survey engineering from the China University of Geosciences (CUG), Wuhan, China, in 2013 and 2017, respectively.

Since 2017, he has been a Lecturer with the Geomatic Engineering Department, University of Mines and Technology (UMaT), Twarka, Ghana. He has authored more than 45 peer-reviewed journal articles. His research interests include application of artificial intelligence in engineering, 2-D/3-D coordinate transformation, height systems, gravity field modeling, and geodetic deformation modeling.

Dr. Ziggah was a recipient of the UMaT staff development fund, Ghana Government Scholarship, and Chinese Government Scholarship to pursue Master and Doctorate degrees. He was awarded the second best paper at the Geographic Information System, Geodesy and Survey Engineering Conference in 2015 at Changsha, China.